Global Optimization of Reverse Osmosis Network for Wastewater Treatment and Minimization

ARTICLE *in* INDUSTRIAL & ENGINEERING CHEMISTRY RESEARCH · APRIL 2008

Impact Factor: 2.59 · DOI: 10.1021/ie071316j

3 AUTHORS, INCLUDING:

Yousef Saif
Petroleum Institute (UAE)
16 PUBLICATIONS **110** CITATIONS
SEE PROFILE

A. Elkamel
University of Waterloo
305 PUBLICATIONS **2,144** CITATIONS
SEE PROFILE

Global Optimization of Reverse Osmosis Network for Wastewater Treatment and Minimization

Yousef Saif, Ali Elkamel,* and Mark Pritzker

Chemical Engineering Department, University of Waterloo, Waterloo, Ontario, Canada N2L 3G1

Reverse osmosis (RO) has shown itself to be a viable technology for the treatment and minimization of industrial and domestic wastewater streams. The current research presents a deterministic branch-and-bound global optimization-based algorithm for the solution of the reverse osmosis network (RON) synthesis problem. The mathematical programming model describes the RON through nonconvex mixed-integer nonlinear programs (MINLPs). A piecewise mixed-integer linear program (MILP) is derived based on the convex relaxation of the nonconvex terms present in the MINLP formulation to approximate the original nonconvex program and to obtain a valid lower bound on the global optimum. The MILP model is solved at every node in the branch-and-bound tree to verify the global optimality of the treatment network within a pre-specified gap tolerance. Several constraints are developed to simultaneously screen the treatment network alternatives during the search, tighten the variable bounds, and consequently accelerate algorithm convergence. Water desalination is considered as a case study to illustrate the global optimization of the RO network.

1. Introduction

Water and wastewater streams are typically contaminated with several pollutants (e.g., organic, inorganic and biological contaminants). Direct discharge of wastewater streams without proper treatment has a drastic impact on the environment. Therefore, wastewater treatment has become an important task, to comply with the strict environmental regulations that are concerned with pollution prevention and public health.

Reverse osmosis (RO) is a pressure-driven process in which a membrane acts as a barrier to retain pollutants in a concentrated stream and allow water to permeate into another purified stream. RO membranes have the ability to retain molecules and ions, because of their small pore size. In addition, RO systems are modular, compact, and consume only moderate amounts of energy during operation. These and other advantages have enabled RO to become a commonly used treatment method and is highly competitive, compared to other separation processes.

The most common practice in optimizing water/wastewater treatment has been through a centralized approach in which several wastewater streams are collected, mixed, and directed to central treatment facilities. Unfortunately, such strategy has proven to be more costly than decentralized approaches. Decentralized treatment involves the multiplicity of the wastewater streams as distinct streams with multiple pollutants. The treatment network is normally represented by the mixing, splitting, and bypass of different streams in a representation that accommodates all possible treatment alternatives (a superstructure). A mathematical programming model based on this superstructure can be formulated to sort all the possible alternatives for minimizing the total wastewater treatment cost.

A RO network is a nonisobaric system in which pumps deliver kinetic energy to wastewater streams, turbines extract energy from reject streams, and RO stages perform the separation of wastewater streams. El-Halwagi gave an adequate superstructure of the RO network problem based on the state space approach.[1] This author subsequently extended this method to hybrid RO networks by combining the RO superstructure with other conventional separation processes.[2] RO and hybrid RO networks are formulated as a nonconvex mixed-integer nonlinear program (MINLP). Vyhmeister et al. applied a genetic algorithm for the superstructure presented by El-Halwagi.[3] However, the execution time for the algorithm was prohibitively long when a large number of unit operations were considered in the superstructure. Saif et al. provided another representation of the RO network, where several alternatives of the superstructure can be safely dropped prior to the optimization task.[4] They also provided mathematical programming-based heuristics to explore the search space of the mathematical program and improve the search for local optimal solutions.

Zhu et al. solved a scheduling problem of a flexible RO network for seawater desalination.[5] The RO design model accounted for the decline in permeate flux, which was due to fouling with an exponential decay function. Several predetermined schedules for membrane regeneration were specified. For each schedule, an optimal network was designed to meet several operating targets. The overall minimum total annualized cost of the network generated from all the schedules was chosen to be the best configuration of the RO-network. Maskan et al. optimized a two-stage RO network for the desalination of brackish water and seawater.[6] Their model for the RO modules accounted for pressure losses that were due to friction and flow in the module manifolds and the effect of concentration polarization to better estimate the osmotic pressure. The objectives of the study were to determine the optimum RO module dimensions and the optimum layout of the treatment network.

In this work, we formulate the RO design network based on a superstructure, which embeds all possible alternatives of a potential treatment network for water and wastewater streams. The superstructure is presented after screening the network alternatives as proposed by Saif et al.[4] It contains several units of pumps, turbines, and RO stages. The mathematical programming model is formulated as a nonconvex MINLP. The nonconvexity of the model results from the bilinear terms that

* To whom correspondence should be addressed. E-mail address: aelkamel@uwaterloo.ca.

10.1021/ie071316j CCC: $40.75
Published on Web 04/05/2008

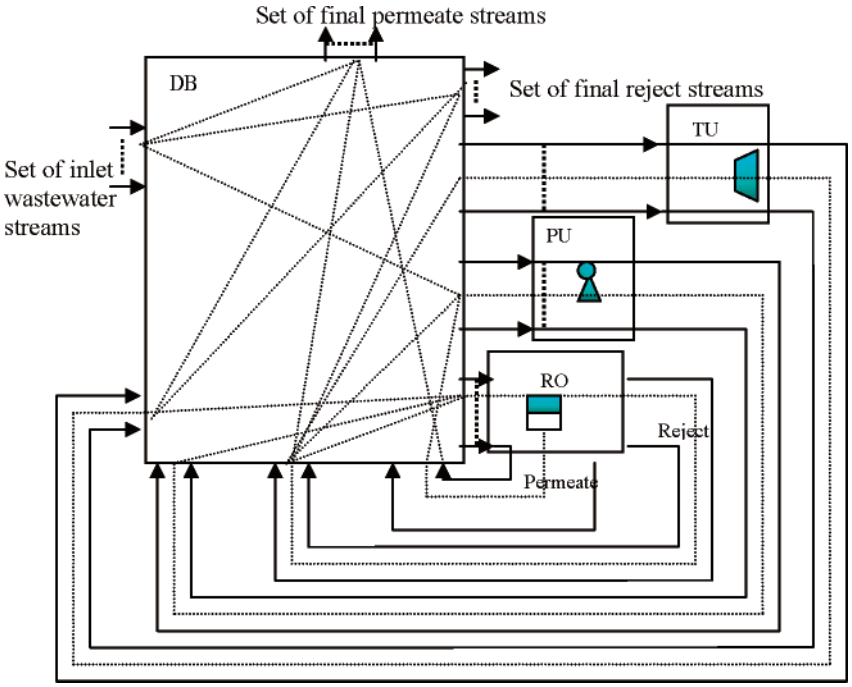

Figure 1. Superstructure representation showing all possible alternatives for the RO network layout.

are present in the constraint set and concave functions in the objective function. Further tightening of the mathematical program is achieved by deriving additional constraints that exploit the mathematical programming structure and the RO network conceptual design. This study extends our previous one[4] by applying an efficient branch-and-bound algorithm to obtain the global optimum for the design and layout of the RO network.

In this sequel, section 2 presents the superstructure description. Section 3 follows with the formulation of the mathematical model. In section 4, the bounding problem of the mathematical program (a mixed-integer linear program, MILP) is derived based on the convex relaxation of the mathematical program. Section 5 gives the mathematical program tightening constraints, and section 6 describes the spatial branch-and-bound algorithm. In section 7, a water desalination case study is presented to illustrate the proposed algorithm. Finally, conclusions of the paper are given in section 8.

2. Superstructure

The RO network has the ability to accommodate multiple wastewater streams with multiple pollutants. It is assumed that the network consists of three different types of unit operations. Pumps are necessary to increase the pressure of different wastewater streams. Each RO stage separates a single feed into a concentrated stream and a diluted stream and is assumed to contain parallel RO modules that are operating under identical conditions. Turbines serve as units to recover kinetic energy from high-pressure streams. With the view of a superstructure, one should allow all possible connections between the unit operations, the unit-operation exit streams, and the inlet wastewater streams entering the network. Figure 1 depicts the proposed superstructure of the RO treatment network previously given by Saif et al.[4]

The superstructure is split into two parts: a distribution box (DB), where mixing/splitting of the streams occur, and unit operation boxes, which alter the feed stream conditions. The following sets are defined to explain the stream assignments within the DB:

SIN = {1, 2, ..., *in*, ...}: set of inlet wastewater streams

SPU = {1, 2, ..., *pu*, ...}: set of pumps in the superstructure

STU = {1, 2, ..., *tu*, ...}: set of turbine units

SRO = {1, 2, ..., *ro*, ...}: set of RO stages

SROREJ = {1, 2, ..., *rorej*, ...}: set of reject streams from the SRO

SROPER = {1, 2, ..., *roper*, ...}: set of permeate streams from the SRO

SFPER = {1, 2, ..., *fper*, ...}: set of final permeate streams

SFREJ = {1, 2, ..., *frej*, ...}: set of final reject streams

SC = {1, 2, ..., *c*, ...}: set of components present in each wastewater stream

By definition, the number of the elements in SROREJ and SROPER is the same as that in SRO. Each inlet wastewater stream F_{in} is split over the sets SPU, SFREJ, and SFPER. The streams F_{in-pu} represent a stream assignment from the wastewater stream *in* to pump node *pu*. We allow for the possibility that not all of each wastewater stream is processed, and, therefore, streams $F_{in-frej}$ and $F_{in-fper}$ provide the option of bypassing the network.

At every pump *pu*, streams F_{in-pu}, $F_{rorej-pu}$, and $F_{roper-pu}$ may mix before the pressurization process. Mixing stream $F_{roper-pu}$ with streams F_{in-pu} and $F_{rorej-pu}$ will reduce the osmotic pressure of the pump-inlet stream. However, mixing may not be economical in the case where some of the $F_{rorej-pu}$ and/or F_{in-pu} streams are highly polluted. If this situation arises, the set of

$F_{roper-pu}$ streams will be processed separately, to reduce the treatment cost.

After the pressurization process, every pump-exit stream F_{pu} is split into F_{pu-ro} streams and distributed over the RO stages SRO. Separation by each RO stage *ro* yields a permeate stream F_{roper} and a reject stream F_{rorej}. The permeate stream F_{roper} is split into two subset streams: $F_{roper-pu}$ loops back to all the pump nodes SPU, whereas $F_{roper-fper}$ contributes to the final permeate product streams F_{FPER}. On the other hand, the reject stream F_{rorej} is split into four subset streams: $F_{rorej-ro}$, $F_{rorej-pu}$, $F_{rorej-tu}$, and $F_{rorej-frej}$. $F_{rorej-ro}$ provides the option of processing reject streams in subsequent RO stages when their pressure remains sufficiently high. $F_{rorej-pu}$ streams flow to the pumping node to increase their pressure. $F_{rorej-tu}$ represents streams that are fed to turbines *STU* for recovery of kinetic energy. Finally, the $F_{rorej-frej}$ streams are included to provide exit streams from the network. The discharge stream F_{tu} from the turbines is split into three streams: F_{tu-ro}, to allow for additional processing in the RO stages, and $F_{tu-fper}$ and $F_{tu-frej}$, for the option of leaving the treatment network.

3. Model Formulation (MINLP)

The objective function of the mathematical model is defined to minimize the total annual cost (TAC) of the unit operations:

$$\mathrm{Min\ TAC} = \sum_{\mathrm{SPU}}^{\mathrm{SRO}} a_{ro,m}\mathrm{NMd}_{ro} + \sum_{\mathrm{STU}}^{\mathrm{SPU}} a_{pu,\mathrm{fx}}\,\mathrm{PPu}_{pu}^{\alpha_{pu}} + \sum^{\mathrm{SPU}} a_{pu,\mathrm{op}}\mathrm{PPu}_{pu} + \sum^{\mathrm{STU}} a_{tu,fx}\,\mathrm{PTu}_{tu}^{\alpha_{tu}} - \sum^{\mathrm{STU}} a_{tu,\mathrm{op}}\mathrm{PTu}_{tu} \quad (1)$$

The cost of each RO stage SRO varies linearly with the number of modules (NMd_{ro}) in the stage, through the parameter $a_{ro,m}$. The pump and turbine fixed costs are given by the power produced/recovered (PPu_{pu}, PTu_{tu}) at every pump or turbine stage (*pu*, *tu*) raised to a fractional constant (α_{pu}, α_{tu}), respectively. The parameters $a_{pu,fx}$ and $a_{tu,fx}$ give the fixed-cost coefficients for the pump and turbine stages, respectively. The pump operational cost and the turbine operational value are assumed to be linear functions, with respect to the power consumption/recovery of the unit through the constants $a_{pu,\mathrm{op}}$ and $a_{tu,\mathrm{op}}$.

The power PPu_{pu} that is required by any pump *pu* is the pressure difference across the unit (ΔP_{pu}) multiplied by the total flow through the unit (F_{pu}), i.e.,

$$\mathrm{PPu}_{pu} = F_{pu}\,\Delta P_{pu} \qquad \forall pu \quad (2)$$

A binary variable y_{pu} defines the existence of a pump if the pressure difference across the unit is nonzero:

$$\Delta P_{pu} \le \Delta P_{pu}^{\mathrm{UP}} y_{pu} \qquad \forall pu \quad (3)$$

Similarly, the power PPu_{tu} that is recovered by turbine *tu* is given by eq 4, and the existence of a turbine within the network is related to a binary variable y_{tu}, as shown in eq 5:

$$\mathrm{PPu}_{tu} = F_{tu}(-\Delta P_{tu}) \qquad \forall tu \quad (4)$$

$$-\Delta P_{tu} \le \Delta P_{tu}^{\mathrm{UP}} y_{tu} \qquad \forall tu \quad (5)$$

The permeate production F_{roper} from a RO stage *ro* is described by a short-cut model presented by Evangellsta.[7] This model relates the permeate flow to the pressure drop across the module ΔP_{ro}, osmotic pressure π_{ro} at the RO-reject side, and the total number of parallel modules present in a stage as follows:

$$F_{roper} = \mathrm{NMd}_{ro} \times W \times \mathrm{SA} \times \gamma(\Delta P_{ro} - \pi_{ro}) \qquad \forall ro \quad (6)$$

$$\gamma = \frac{\eta}{1 + [16 \times W \times \mu \times r_o \times ll_s \times (\eta/r_i^4)]} \quad (7)$$

$$\eta = \frac{\tanh\{[16 \times W \times \mu \times (r_o/r_i^2)]^{1/2}(l/r_i)\}}{[16 \times W \times \mu \times (r_o/r_i^2)]^{1/2}(l/r_i)} \quad (8)$$

where W is the water permeability coefficient, SA the RO module surface area, and γ a parameter related to the RO module dimension and water properties. The concentration $X_{c,roper}$ of a component in any permeate stream is related to its average concentration $X_{c-\mathrm{avg},ro}$ on the feed side of the RO module, the solute permeability coefficient K_c, the pressure drop ΔP_{ro} across the RO membrane, the water permeability coefficient, and the geometrical parameter γ, as given in eq 9:

$$X_{\mathrm{c},roper} = \frac{K_c X_{c-\mathrm{avg},ro}}{W\gamma(\Delta P_{ro} - \Delta\pi_{ro})} \qquad \forall c,ro \quad (9)$$

The total number of modules NMd_{ro} present in any RO stage *ro* is an integer variable. However, to simplify the permeate balance in eq 6, fractional values of NMd_{ro} are permitted for the purpose of estimating the RO stage surface area. This assumption is reasonable to reduce the complexity of the mathematical program. The osmotic pressure π_{ro} at every RO stage is approximated by a rule of thumb[8] for dilute solutions:

$$\pi_{ro} = \mathrm{OS}\sum^{c} X_{c-\mathrm{avg},ro} \qquad \forall ro + \in \mathrm{SRO} \quad (10)$$

where OS is a proportionality constant between the osmotic pressure and average solute concentration on the feed side. The solute concentration of the permeate is so much lower than that on the feed side that its osmotic pressure is neglected in calculating $\Delta\pi_{ro}$.

The existence of a RO stage *ro* is indicated when the binary variable y_{ro} has a value of 1. Permeate production in stage *ro* is related to this binary variable by eq 11:

$$\mathrm{Fp}_{ro} \le F_{ro}^{\mathrm{UP}}\, y_{ro} \qquad \forall ro \quad (11)$$

RO module operation may require bounds on the operational variables to improve the system performance. Equation 12 enforces that the inlet flowrate to any RO stage be bounded between upper and lower limits. A lower limit is specified to avoid excessive concentration polarization, while the upper limit is governed by considerations that are related to pump operation and the overall feed rate of the wastewater to the network. Also, the inlet feed pressure to any RO stage may not exceed an upper value, as described in eq 13:

$$F_{ro}^{\mathrm{LO}}\mathrm{NMd}_{ro} \le F_{ro} \le F_{ro}^{\mathrm{UP}}\mathrm{NMd}_{ro} \qquad \forall ro \quad (12)$$

$$P_{ro} \le P_{ro}^{\mathrm{UP}} \qquad \forall ro \quad (13)$$

Conservation of water and solute species in each RO stage are described by eqs 14 and 15, i.e.,

$$F_{ro} = F_{roper} + \mathrm{Fr}_{rorej} \qquad \forall ro \quad (14)$$

$$F_{ro}X_{c,ro} = F_{roper}X_{c,roper} + F_{rorej}X_{c,rorej} \qquad \forall c,ro \quad (15)$$

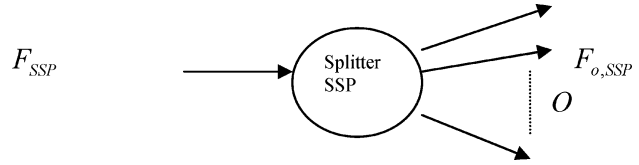

Figure 2. Inlet and exit stream conditions for a splitter unit.

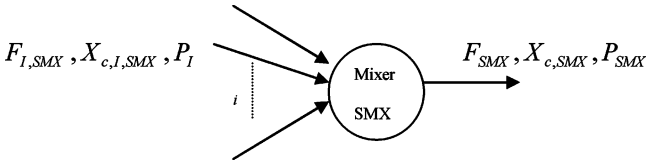

Figure 3. Inlet and exit conditions for a mixer unit.

The DB contains several splitting nodes (e.g., SIN, SROPER, SROREJ, SPU, STU). Figure 2 shows a splitter node, $sp \in$ SSP, where a single feed stream F_{sp} is split to several exit streams $F_{o,sp}$. Equation 16 gives the total water balance over the splitter node:

$$F_{sp} = \sum^{O} F_{o,sp} \qquad \forall sp \tag{16}$$

A mixing node, $mx \in$ SMX (e.g., SRO, SPU, STU, SFPER, SFREJ), is represented by Figure 3, where several streams $F_{i,mx}$ are mixed to yield a single stream F_{mx}. Water and component balances over the mixer node are given by eqs 17 and 18:

$$F_{mx} = \sum^{I} F_{i,mx} \qquad \forall mx \tag{17}$$

$$F_{mx} X_{c,mx} = \sum^{I} F_{i,mx} X_{c,mx} \qquad \forall c,mx \tag{18}$$

Furthermore, it is assumed that mixing is not allowed between streams that have different pressure values. This condition is enforced by eqs 19−21, through a binary variable $y_{i,mx}$, which forces the flow of stream i to vanish if its pressure does not match that of the mixer discharge.

$$P_{mx} - P_{i,mx} \le M(1 - y_{i,mx}) \qquad \forall i,mx \tag{19}$$

$$P_{mx} - P_{i,mx} \ge -M(1 - y_{i,mx}) \qquad \forall i,mx \tag{20}$$

$$F_{mx} \le F_{i,mx}^{\mathrm{UP}} y_{i,mx} \qquad \forall i,mx \tag{21}$$

Other constraints are imposed on the exit streams from the network. Equation 22 prescribes that the flow rate of the final permeate streams not be less than a minimum value F_{fper}^{LO}. Environmental constraints require that the pollutant concentration $X_{c,fper}$ not exceed a threshold discharge $X_{c,fper}^{\mathrm{UP}}$ (see eq 23).

$$F_{fper} \ge F_{fper}^{\mathrm{LO}} \qquad \forall fper \tag{22}$$

$$X_{c,fper} \le X_{c,fper}^{\mathrm{UP}} \qquad \forall c,fper \tag{23}$$

4. Convex Relaxation of the Nonlinear Model

Branch-and-bound global search algorithms usually approximate nonconvex systems using functions that bound the nonconvex function values over their intervals. For a minimization problem, a concave function $\psi(z)^{\alpha}$ that is defined in the objective function is replaced by a chord line $\underline{\psi}(z)$, which is defined by eq 24 as an underestimate:

$$\underline{\psi}(z) \ge (\psi(z)^{\mathrm{LO}})^{\alpha} + \left(\frac{(\psi(z)^{\mathrm{UP}})^{\alpha} - (\psi(z)^{\mathrm{LO}})^{\alpha}}{z^{\mathrm{U}} - z^{\mathrm{L}}}\right)(z - z^{\mathrm{L}}) \tag{24}$$

For a bilinear function $\chi = qw$, the convex/concave envelopes are given by the McCormick inequalities:[9]

$$\left.\begin{aligned} \chi &\ge q^{\mathrm{LO}} w + q w^{\mathrm{LO}} - q^{\mathrm{LO}} w^{\mathrm{LO}} \\ \chi &\ge q^{\mathrm{UP}} w + q w^{\mathrm{UP}} - q^{\mathrm{UP}} w^{\mathrm{UP}} \\ \chi &\le q^{\mathrm{LO}} w + q w^{\mathrm{UP}} - q^{\mathrm{LO}} w^{\mathrm{UP}} \\ \chi &\le q^{\mathrm{UP}} w + q w^{\mathrm{LO}} - q^{\mathrm{UP}} w^{\mathrm{LO}} \end{aligned}\right\} \tag{25}$$

The convexification of the MINLP model yields a MILP model that bounds the global optimum. Sherali and Alameddine tackled general bilinear programs, using the concepts of the Reformulation−Linearization Technique (RLT).[10] The technique generates redundant equations in the relaxed problem, with respect to the nonconvex program by a multiplication process. Such a technique adds a large number of nonredundant constraints in the relaxed problem, which helps tighten the MILP model. Alternatively, a tighter MILP model can be constructed by introducing binary variables to formulate a piecewise discrete approximation of every nonconvex term interval.[11,12]

A concave function $\psi(z)^{\alpha}$ can be further approximated by partitioning its independent variable into DIS1 subintervals and approximating the function by its underestimate over all the subintervals, as[12]

$$z = \sum_{\mathrm{dis1}=1}^{\mathrm{DIS1}} z_{\mathrm{dis1}} \tag{26}$$

$$\psi(z) = \sum_{\mathrm{dis1}=1}^{\mathrm{DIS1}} \psi(z)_{\mathrm{dis1}} \tag{27}$$

$$\underline{\psi}(z) \ge \sum_{\mathrm{dis1}=1}^{\mathrm{DIS1}} (\psi(z)_{\mathrm{dis1}}^{\mathrm{LO}})^{\alpha} \omega_{\mathrm{dis1}} + \left(\frac{(\psi(z)_{\mathrm{dis1}}^{\mathrm{UP}})^{\alpha} - (\psi(z)_{\mathrm{dis1}}^{\mathrm{LO}})^{\alpha}}{z_{\mathrm{dis1}}^{\mathrm{U}} - z_{\mathrm{dis1}}^{\mathrm{L}}}\right)(z_{\mathrm{dis1}} - z_{\mathrm{dis1}}^{\mathrm{L}} \omega_{\mathrm{dis1}}) \tag{28}$$

$$z_{\mathrm{dis1}}^{\mathrm{LO}} \omega_{\mathrm{dis1}} \le z_{\mathrm{dis1}} \le z_{\mathrm{dis1}}^{\mathrm{UP}} \omega_{\mathrm{dis1}} \tag{29}$$

$$\psi(z)_{\mathrm{dis1}}^{\mathrm{LO}} \omega_{\mathrm{dis1}} \le \psi(z)_{\mathrm{dis1}} \le \psi(z)_{\mathrm{dis1}}^{\mathrm{UP}} \omega_{\mathrm{dis1}} \tag{30}$$

$$\sum^{\mathrm{DIS1}} \omega_{\mathrm{dis1}} = 1 \tag{31}$$

The domains of the independent variable z and dependent variable $\psi(z)$ are split into DIS1 subintervals (eqs 26 and 27), where the variables z_{dis1} and $\psi(z)_{\mathrm{dis1}}$ cover the z and $\psi(z)$ values in the subinterval dis1, respectively. Equation 28 defines the DIS1 chord lines for the concave function in its domain. The binary variables ω_{dis1} ensure that $z_{\mathrm{dis1}}$and $\psi(z)_{dis1}$ lie within the appropriate intervals through eqs 29−31.

For a bilinear function $\chi = qw$, the domains of the variables q and w are divided into DIS2 and DIS3 subintervals, i.e., eqs 32 and 33:

$$q = \sum_{\mathrm{dis2}=1}^{\mathrm{DIS2}} q_{\mathrm{dis2}} \tag{32}$$

$$w = \sum_{\mathrm{dis3}=1}^{\mathrm{DIS3}} w_{\mathrm{dis3}} \tag{33}$$

The formulation of a bilinear function after the division process is represented as[12]

$$\left.\begin{aligned}
\chi &\geq \sum_{dis2=1}^{DIS2}\sum_{dis3=1}^{DIS3} q^{LO}_{dis2} w_{dis3} + q_{dis2} w^{LO}_{dis3} - q^{LO}_{dis2} w^{LO}_{dis3} \tau_{dis2,dis3} \\
\chi &\geq \sum_{dis2=1}^{DIS2}\sum_{dis3=1}^{DIS3} q^{UP}_{dis2} w_{dis3} + q_{dis2}\, w^{UP}_{dis3} - q^{UP}_{dis2} w^{UP}_{dis3} \tau_{dis2,dis3} \\
\chi &\leq \sum_{dis2=1}^{DIS2}\sum_{dis3=1}^{DIS3} q^{LO}_{dis2} w_{dis3} + q_{dis2}\, w^{UP}_{dis3} - q^{LO}_{dis2} w^{UP}_{dis3}\, \tau_{dis2,dis3} \\
\chi &\leq \sum_{dis2=1}^{DIS2}\sum_{dis3=1}^{DIS3} q^{UP}_{dis2} w_{dis3} + q_{dis2} w^{LO}_{dis3} - q^{UP}_{dis2} w^{LO}_{dis3} \tau_{dis2,dis3}
\end{aligned}\right\} \quad (34)$$

$$q^{LO}_{dis2,dis3}\tau_{dis2,dis3} \leq q_{dis2,dis3} \leq q^{UP}_{dis2,dis3}\tau_{dis2,dis3} \quad (35)$$

$$w^{LO}_{dis2,dis3}\tau_{dis2,dis3} \leq w_{dis2,dis3} \leq w^{UP}_{dis2,dis3}\tau_{dis2,dis3} \quad (36)$$

$$\sum_{dis2=1}^{DIS2}\sum_{dis3=1}^{DIS3} \tau_{dis2,dis3} = 1 \quad (37)$$

The overestimators/underestimators given in eq 34 are constructed for every subinterval (dis2,dis3). Also, the binary variables $\tau_{dis2,dis3}$ ensure that the values for the continuous variables will be within the appropriate subinterval (dis2,dis3), through eqs 35−37. To avoid introducing a large number of binary variables, the intervals of the flow rate variables in the bilinear functions present in the component balance equations are partitioned. In contrast, the partitioned variables of the bilinear functions involved in the unit operation models are chosen based on the variable that has the larger interval. In the current study, the concave functions represent the fixed cost of the pumps and turbines. The bilinear functions in the mathematical program are the nonconvex terms in the component balance equations and the unit operation model equations.

5. Model Tightening Constraints

In this section, several tightening constraints are presented to improve the relaxed formulation. These constraints are developed for the original MINLP, relaxed MILP, and piecewise discrete MILP formulations.

5.1. MINLP-Based Tightening Constraints. The mixing assumption between the streams at every mixing node (eqs 19−21) can be used to reduce the number of possible stream assignments. The following points explain these tightening constraints:

(1) Because a pressure drop exists at every RO stage, a stream discharged from an RO stage cannot be directly recycled back to the same stage. Consequently, RO-stage reject recycle streams can be dropped from the formulation.

(2) Every existing RO reject stream has possible stream assignments to the turbine stages. In addition, any discharge from a turbine may have directed streams to the RO stages. Therefore, the following constraint can be added to limit the existence of the following streams that are due to the pressure drop in the turbine stage:

$$y_{rorej-tu} + y_{tu-ro} \leq 1 \qquad \forall ro,tu \quad (38)$$

(3) During the solution of the problem, high-pressure streams ($F_{rorej-pu}$) and low-pressure streams (F_{in-pu}, $F_{roper-pu}$) may happen to be directed to the same pump node. To eliminate this possibility, the following constraints are added:

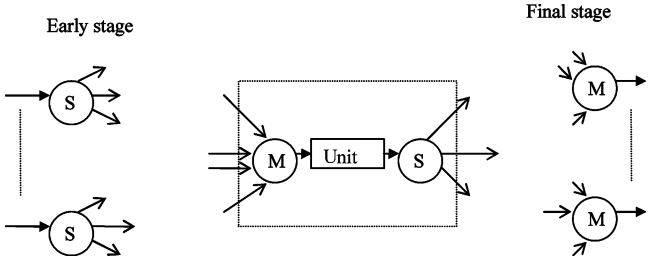

Figure 4. Schematic representation showing an example of the possible linkage between different levels within the superstructure.

$$y_{rorej-pu} + y_{in-pu} \leq 1 \qquad \forall rorej,pu,in \quad (39a)$$

$$y_{rorej-pu} + y_{roper-pu} \leq 1 \qquad \forall rorej,roper,pu \quad (39b)$$

5.2. MILP-Based Tightening Constraints. Generally, replacing the nonconvex terms by their approximated equations gives a loose relaxed model. These nonconvex terms result from the component balance equations at the mixer nodes and the material and the energy balance equations for the unit operations. The addition of redundant equations, with respect to the MINLP formulation, usually improves the MILP relaxation. Thus, the exploitation of other relations (equalities or inequalities) that are related to the component flow and the energy balances in the network will improve the relaxed formulation.

The redundant equations that are based on the component balances are generated to relate the different levels in the network that have no explicit balance equations in the original nonconvex program. Figure 4 shows that the network feed streams are split at an early stage and then are processed sequentially by several units to reach the final product stage. In modeling the MINLP, the relation between different stages are implicitly stated through the model variables and equations. Therefore, the MILP model will not capture all the implicit relations in the original MINLP after the model is made convex. The dashed box in Figure 4 gives an example of deriving additional component balance equations that link mixer and splitter nodes. Consequently, the generation of these equality constraints in the relaxed problem will help to tighten the lower bound.

A tightening constraint set can be derived from energy conservation over the entire network. An additional energy-based constraint that was not needed in the original formulation can be stated as follows:

energy produced by the pump stages =
separation work done by RO stages +
energy recovered by turbines +
energy stored in reject streams comprising
the final reject stream

Other tightening constraints pertain to RO-permeate looping within the network. RO-permeate looping is a definition of the $F_{roper-pu}$ streams that are being processed separately from other wastewater and RO-reject streams. The $F_{roper-pu}$ streams serves one of two objectives: to dilute the inlet wastewater streams F_{in-pu} or to reprocess permeate streams (RO-permeate looping), to reduce costs when treating the RO-reject streams is not economical. The proportion of mixing between $F_{roper-pu}$ and F_{in-pu} prior to any pump node determines whether the resulting stream from mixing is dilute or concentrated.

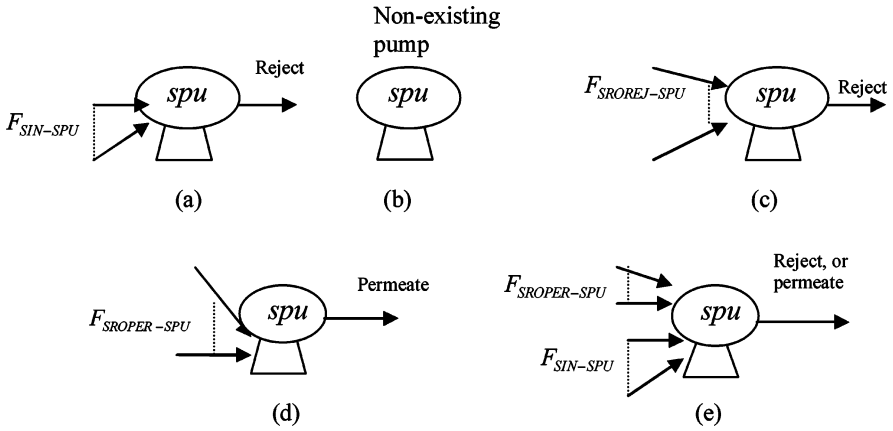

Figure 5. All possible conditions that may occur for streams flowing into a pump present in the treatment network.

Streams $F_{rorej-fper}$ and $F_{tu-fper}$ are included in the superstructure to provide the option of mixing with the final permeate streams only when permeate looping is done. In addition, streams $F_{rorej-fper}$ and $F_{tu-fper}$ should have component concentrations that are close to the upper allowed value (c_{fper}) in the final permeate. However, because of the convexification of the component balance terms, the component balance terms that correspond to the $F_{rorej-fper}$ and $F_{tu-fper}$ streams are underestimated, which satisfies the final permeate flow and concentration requirements, even if no permeate looping is done. To determine whether permeate is being looped, a new binary variable y_{PL} is introduced:

$$y_{\mathrm{PL}} = \begin{cases} 1 & \left(\text{if } \sum^{roper}\sum^{pu} F_{roper-pu} \le 0\right) \\ 0 & (\text{otherwise}) \end{cases} \tag{40}$$

The following inequalities are used to ensure that the condition $\sum^{roper}\sum^{pu} F_{roper-pu} \le 0$ holds:

$$\in + y_{\mathrm{PL}}\left(\sum^{roper}\sum^{pu} F_{roper-pu}\right)^{\mathrm{LO}} \le \sum^{roper}\sum^{pu} F_{roper-pu} \tag{41}$$

$$(1 - y_{\mathrm{PL}})\left(\sum^{roper}\sum^{pu} F_{roper-pu}\right)^{\mathrm{UP}} \ge \sum^{roper}\sum^{pu} F_{roper-pu} \tag{42}$$

The absence of permeate looping implies that the RO-reject streams are processed within the network and the RO-permeate streams are collected to satisfy the final permeate flow and concentration demand. As a result, the streams $F_{rorej-fper}$ and $F_{tu-fper}$ should not be mixed with the final permeate products F_{fper}, because this will significantly increase the permeate product concentration. Mathematically, these conditions are formulated as follows:

$$F_{tu-fper} \le F^{\mathrm{UP}}_{tu-fper}(1 - y_{\mathrm{PL}}) \qquad \forall tu, fper \tag{43}$$

$$F_{rorej-fper} \le F^{\mathrm{UP}}_{rorej-fper}(1 - y_{\mathrm{PL}}) \qquad \forall rorej, fper \tag{44}$$

On the other hand, if any permeate is recycled or reprocessed, eqs 41 and 42 are violated. Figure 5 shows the possible conditions that involve the pump nodes in the network. Because conditions a−c in Figure 5 do not include any permeate stream, only a reject or wastewater stream is discharged from the pump unit. Condition d in Figure 5 depicts the case of permeate looping in the network, whereas condition e in Figure 5 shows two mixing situations:

(1) The value of $\sum^{roper} F_{roper-pu}$ is smaller than $\sum^{in} F_{in-pu}$. This situation corresponds to the case of the treatment of a highly polluted wastewater stream. Therefore, mixing of the RO-permeate stream with the inlet wastewater reduces the osmotic pressure and avoids expensive continuous processing of the RO-reject streams in several RO stages.

(2) The opposite condition to situation 1 (described above) is less likely to happen, because it represents conflict with the objectives of the treatment network.

Therefore, binary variables are introduced to assist in deciding whether mixing yields a stream that can be considered to be a concentrate or permeate at every pump node. For every pumping node, a binary variable is defined as follows:

$$\mathrm{ymix}_{pu} = \begin{cases} 1 & \text{if } \sum^{roper} F_{roper-pu} - \sum^{in} F_{in-pu} \ge \in \\ 0 & (\text{otherwise}) \end{cases} \qquad \forall pu \tag{45}$$

If the inequality holds (i.e., $\sum^{roper} F_{roper-pu} - \sum^{in} F_{in-pu} \ge \in$), the stream passing through the pumping node is considered to be a permeate. Otherwise, the pump exit stream is considered to be a concentrate. Other inequality constraints that have been added to evaluate the previous conditions are given in eqs 46 and 47:

$$\sum^{roper} F_{roper-pu} - \sum^{in} F_{in-pu} - \in \ge -\left(\sum^{in} F_{in-pu}\right)^{\mathrm{UP}}(1 - \mathrm{ymix}_{pu}) \qquad \forall pu \tag{46}$$

$$\sum^{roper} F_{roper-pu} - \sum^{in} F_{in-pu} - \in \le \left(\sum^{roper} F_{roper-pu}\right)^{\mathrm{UP}}\mathrm{ymix}_{pu} - \in \qquad \forall pu \tag{47}$$

It is also valid to state that, if these conditions do not hold for all the pump nodes, then no permeate looping occurs in the network, i.e.,

$$\sum^{pu} \mathrm{ymix}_{pu} + y_{\mathrm{PL}} \ge 1 \tag{48}$$

If permeate looping occurs at a pumping node, this requires that the stream flow be traced through all possible arrangements of the units to derive additional tightening constraints. Within

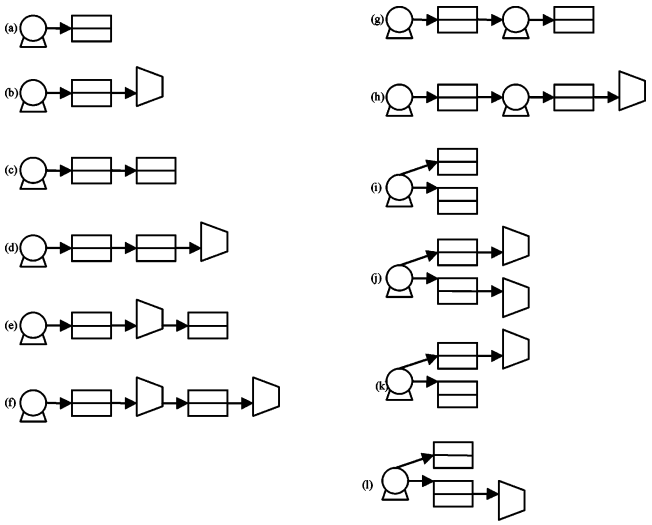

Figure 6. All possible configurations for the sequence of the unit operations considered in the superstructure of the treatment network.

these configurations, the set of streams $F_{rorej-fper}$ and $F_{tu-fper}$ may exist. On the other hand, the presence of a reject stream at a pumping node requires the elimination of the permeate streams from the RO and the turbine stages.

To achieve this objective, binary variables ($y_{rorej-fper}$, $y_{tu-fper}$) are defined for the stream set $F_{rorej-fper}$ and $F_{tu-fper}$ as follows:

$$y_{rorej-fper}, y_{tu-fper} = \begin{cases} 1 & \text{(if a reject or wastewater stream passes through the unit)} \\ 0 & \text{(otherwise)} \end{cases} \quad (49)$$

Additional constraints (eqs 50 and 51) are necessary to eliminate the streams $F_{rorej-fper}$ and $F_{tu-fper}$ whenever the previous conditions hold. Other constraints (eqs 52 and 53) can be added to relate the binary variable y_{PL} to the binary variables $y_{rorej-fper}$ and $y_{tu-fper}$.

$$F_{rorej-fper} \le F^{UP}_{rorej-fper}(1 - y_{rorej-fper}) \qquad \forall rorej,fper \quad (50)$$

$$F_{tu-fper} \le F^{UP}_{tu-fper}(1 - y_{tu-fper}) \qquad \forall tu,fper \quad (51)$$

$$y_{rorej-fper} \ge y_{PL} \qquad \forall rorej,fper \quad (52)$$

$$y_{tu-fper} \ge y_{PL} \qquad \forall tu,fper \quad (53)$$

Figure 6 shows all possible unit arrangements after a stream passes through a pumping node, assuming the existence of a total of six units in the network (e.g., two RO stages, two pumps, and two turbines). Of course, these configurations are defined over the sets SRO, SPU, and STU. The formulation of the tightening constraints (eq 54) is developed as a logical proposition, based on the conditions necessary for the nonexistence of permeate recycling at a pump, stream assignments among the unit operations, and elimination of the stream sets $F_{rorej-fper}$, and $F_{tu-fper}$. The parameter y_{unit} represents the binary variables $y_{rorej-fper}$ and $y_{tu-fper}$. These logical propositions can be transformed to linear inequalities, following the DeMorgan transformation. As an example, Figure 7 presents the constraints for configuration c that has been shown in Figure 6, defined over the sets SRO and SPU. It gives all their constraints, assuming that the final permeate stream set has a single element.

$$\begin{cases} \neg ymix_{pu} \wedge \overbrace{y_{unit1-unit2} \ldots\ldots \wedge y_{unit\,x-unit\,y}} \Rightarrow y_{unit1-fper} \\ \vdots \\ \vdots \\ \neg ymix_{pu} \wedge y_{unit1-unit2} \ldots\ldots \wedge y_{unit\,x-unit\,y} \Rightarrow y_{unit\,x-fper} \\ \neg ymix_{pu} \wedge y_{unit1-unit2} \ldots\ldots \wedge y_{unit\,x-unit\,y} \Rightarrow y_{unit\,y-fper} \end{cases} \quad \forall pu \quad (54)$$

5.3. Piecewise Discrete MILP-Based Tightening Constraints. The solution of the piecewise discrete MILP model at every node in the branch-and-bound tree requires extensive computations. To accelerate the convergence of the branch-and-bound tree, other tightening equations are added to the model. These equations represent relations between the binary variables based on the discussion in sections 4, 5.1, and 5.2.

For nonexistent unit operations and stream assignments within the DB, the optimal values for their operation conditions and flow variables must be in the first sub-divided interval. A set of relations can be established between the pump/turbine-binary variable and the binary variables that appear in eq 31 as follows:

$$y_{pu} + \omega_{dis1} \ge 1 \qquad \forall pu, dis1 = 1 \quad (55)$$

$$y_{tu} + \omega_{dis1} \ge 1 \qquad \forall tu, dis1 = 1 \quad (56)$$

$$y_{pu} \ge \omega_{dis1} \qquad \forall pu, dis1 \ne 1 \quad (57)$$

$$y_{tu} \ge \omega_{dis1} \qquad \forall pu, dis1 \ne 1 \quad (58)$$

Similarly, other relations can be derived for the bilinear functions that represent component balance terms and energy balance equations for the unit operations. Equations 59 and 60 give these relations for the stream assignments in the DB as

$$y_{stream} + \tau_{dis2,dis3} \ge 1 \qquad \forall stream, dis2 = 1, dis3 = 1 \quad (59)$$

$$y_{stream} \ge \tau_{dis2,dis3} \qquad \forall stream, dis2 \ne 1, dis3 \ne 1 \quad (60)$$

Other relations can also be established for the binary variables y_{PL}, $ymix_{pu}$, $y_{rorej-fper}$, and $y_{tu-fper}$ to obtain additional constraints that are similar to the previous constraints.

6. Spatial Branch and Bound Algorithm

The branch-and-bound algorithm consists of the following steps:

(1) Preprocessing: After screening the decision variable bounds, the heuristic approach given by Saif et al.[4] is applied to obtain a valid overall upper bound (OUB) of the MINLP model. The MINLP model can also be solved locally, using any MINLP commercial software.

(2) Contraction: Within the branch-and-bound tree, the variable upper and lower bounds can be further optimized based on the following sub-optimization problems:

$$\text{Min/Max } \kappa$$

$$\text{s.t.}$$

$$\text{relaxed problem constraint set}$$

$$\text{OBJ} \le \text{OUB}$$

where κ represents the independent variables that are involved in any nonconvex term given by the MINLP model. In this study, contraction is applied to the flow rate variables in the

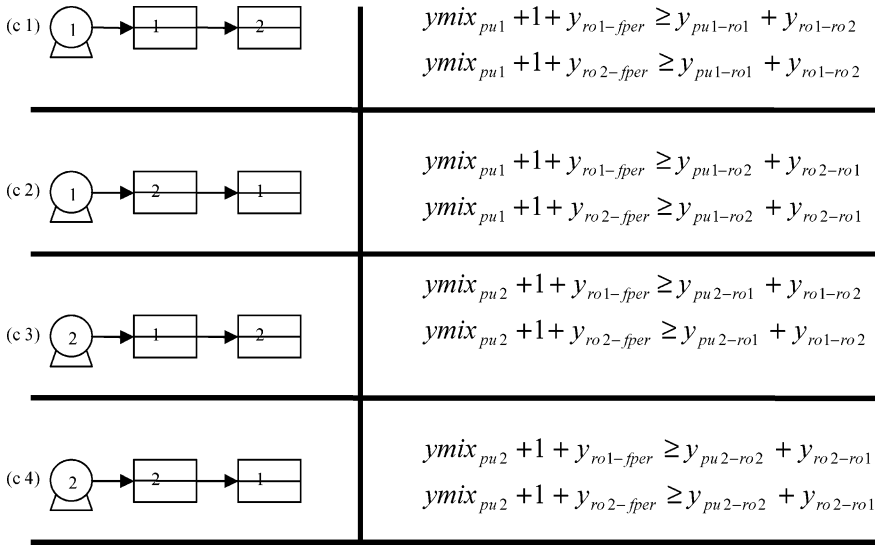

Figure 7. All possible arrangements and corresponding logical constraints associated with configuration c of Figure 6.

Table 1. Geometrical Properties of DuPont RO Modules and Their Dimensions

module properties	B-10 (desalination case)	B-9 (pulp and paper case)
fiber length, l	0.75 m	0.75 m
fiber seal length, l_s	0.075 m	0.075 m
outer radius of fiber, r_o	50×10^{-6} m	42×10^{-6} m
inner radius of fiber, r_i	21×10^{-6} m	21×10^{-6} m
membrane area, SA	152 m^2	180 m

network and all the variables included in any nonconvex term present in the unit models.

(3) Upper bounding step: The binary variable values (stream assignments, unit operations) from the discrete MILP model solution are fixed in the MINLP to generate a NLP problem. When the NLP problem is solved, a new OUB may be found.

(4) Node fathoming: Any node in the branch-and-bound tree can be fathomed either if the node lower bound (LB) is greater than the OUB or if the node gap is less than some tolerance ϵ. The node gap is defined as

$$\mathrm{Gap}_{\mathrm{node}} = \begin{cases} \left|\dfrac{\mathrm{OUB} - \mathrm{LB}}{\mathrm{OUB}}\right| & (\text{if OUB} \neq 0) \\ -\mathrm{LB} & (\text{if OUB} = 0) \end{cases}$$

examination of the branch-and-bound tree can be stopped whenever all the open nodes are fathomed.

(5) Spatial branch-and-bound: Node selection in the branch-and-bound tree seeks a node with the lowest lower bound. Upon solution of the current node, the mother node can be divided into two other open nodes, after selection of a branching variable if the node gap is greater than the tolerance. The branching variable is chosen to be in a nonconvex term, where the absolute value difference between the nonconvex term and its approximation is the largest among all the model nonconvex terms. This variable will also be the one with the largest interval value in this nonconvex term. The bisection rule is picked as a division point for the branching variable.

7. Case Study

This section applies the concepts that have been presented in the previous sections on a case study involving the desalination of a single seawater stream by hollow-fiber DuPont B-10 RO modules. All the cost parameters and unit operation parameters were taken from Elhalwagi.[1] Table 1 presents the geometrical properties of DuPont hollow-fiber RO modules, and Table 2 lists the cost coefficients for the unit operations. The MILP and NLP were solved using the CPLEX and CONOPT 3 packages in GAMS 22.5, respectively.[13] The program was run on a Pentium IV personal computer with a 2.8 GHz CPU and 1 GB of memory. Input data for the optimization problem are given in Table 3. The superstructure includes two RO stages, two pumps, and two turbine stages.

The resulting mathematical program contains 30 binary variables, 123 continuous variables, 112 nonconvex terms, and 156 constraints. In the formulation of the piecewise discrete MILP model (see section 4), all the nonconvex term variable intervals are divided into four equal intervals (see eqs 26−37). For every node in the branch-and-bound tree, the node gap is compared to a tolerance of $\epsilon = 0.03$. The contraction problems are solved for the first three nodes within the branch-and-bound tree.

By applying the proposed algorithm, the global solution was verified by exploring only seven nodes in the branch-and-bound tree. An execution time of 643.3 CPU s was required to obtain the global optimum for the case study. The effects of the tightening constraints on the efficiency of the algorithm and the solution time are worth noting. A lower bound that showed no improvement was observed during the search when the tightening constraints were dropped from the relaxed formulation. They significantly improved the contraction routine, variable bound updates, and, consequently, the required execution time of the algorithm.

The globally optimum RO network for the desalination case study was found by the heuristic search to require a treatment cost of $230 906/yr. Figure 8 presents the layout of the global solution for this network. The optimum layout includes two RO stages in series, a pump prior to the first RO stage, a booster pump between RO stages, and a turbine, following the second RO stage, to extract energy from the second-stage reject stream. One of the turbines included in the superstructure was not needed. The optimum layout results in a cascade configuration with 55 modules

Table 2. Cost Coefficients for the Unit Operations[12]

coefficient	definition	units	seawater desalination case	pulp and paper case
a_{MRO}	includes the annualized installation cost of the RO module, membrane regeneration, labor, and maintenance	$/(module yr)	1450	1140
$a_{Pu,f}$	fixed cost of the pump installation	$/(((kg/s) bar)$^{0.79}$ yr)	139.93	139.93
$a_{Pu,o}$	operating cost of the pump	$/(((kg/s) bar) yr)	80	80
$a_{Tu,f}$	fixed cost of the turbine installation	$/(((kg/s) bar)$^{0.47}$ yr)	93.62	93.62
$a_{Tu,o}$	operating cost of the turbine	$/(((kg/s) bar) yr)	34	34

Table 3. Input Data for the Seawater Desalination Case

parameter	value
seawater feed flow rate	19.29 kg/s
feed composition	0.0348
minimum final permeate flow rate	5.787 kg/s
maximum final permeate composition	0.00057
minimum flow rate per module	0.21 kg/s
maximum flow rate per module	0.27 kg/s
maximum feed pressure	68.88×10^5 Pa
pressure drop per module	0.22×10^5 Pa
pure water permeability, W	1.2×10^{-10} kg/(s N)
solute transport parameter, K_c	4.0×10^{-6} kg/(m^2 s)

in parallel in the first RO stage and 45 modules in the second stage. The RO-permeate streams are continuously collected and combined to supply the final permeate product for the network. The most interesting feature of the design is the bypass of a significant portion of the inlet feed seawater from the treatment train directly to the final reject stream, where it is combined with the portion of the inlet that was treated and rejected. This significantly reduces the load on the downstream units and, consequently, the treatment costs. A portion of the inlet stream is bypassed directly to the final permeate stream, but the amount is very small.

For the purposes of comparison, the process layout obtained by El-Halwagi[1] for the same case study is presented in Figure 9. The difference in these results, relative to those in Figure 8, demonstrates the advantage of obtaining a global optimum solution using the branch-and-bound algorithm. The optimum treatment cost obtained in the current study by the branch-and-bound algorithm is 14.8% lower than the cost of $270 868/yr that was reported by El Halwagi.[1] Comparison of Figures 8 and 9 shows that the main reason for this difference is that a significant feature of the circuit layout obtained by the branch-and-bound method is a direct bypass of a portion of the inlet

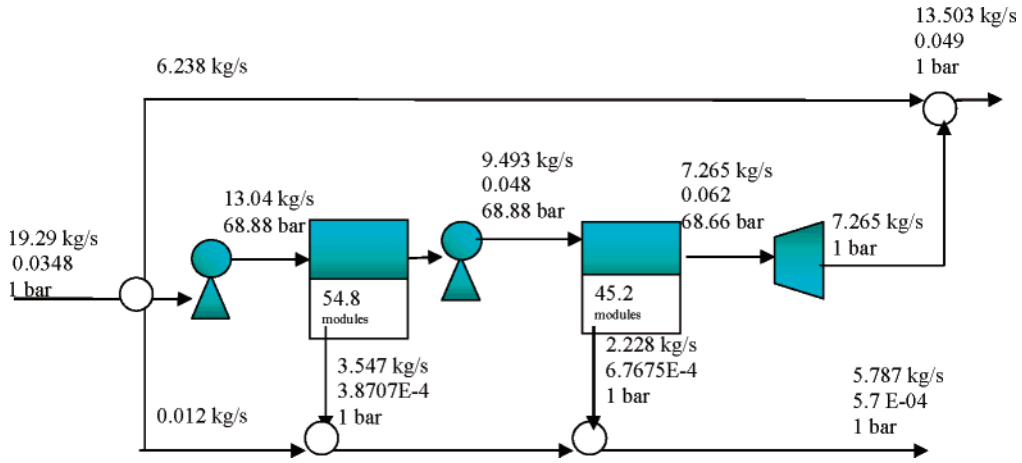

Figure 8. Globally optimum design and operating conditions for the RO network for the seawater desalination case study.

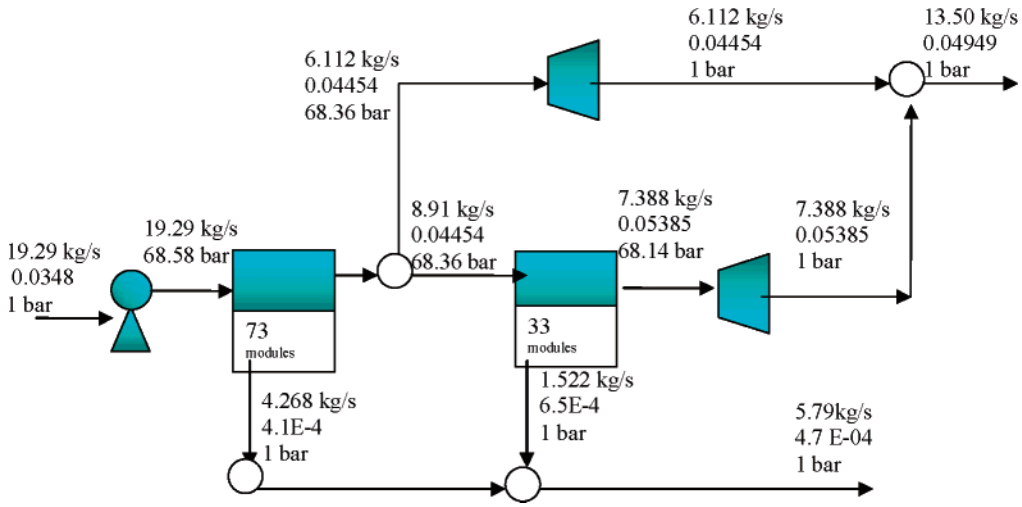

Figure 9. Optimal design and operating conditions for the RO network obtained by El Halwagi[1] for the seawater desalination study.

feed stream to the final reject stream, whereas the circuit design reported by El Halwagi[1] does not include this feature. This effectively reduces the mass flow rate of the inlet stream that must be treated by RO according to the solution obtained by the branch-and-bound method, which leads to significantly fewer membrane modules being required in the first RO stage and lower treatment costs.

8. Conclusion

The search for a globally optimal design and operation of a reverse osmosis (RO) network was addressed for the treatment of water and industrial wastewater streams. A superstructure is assumed to embed all possible alternatives and encompass a hidden optimum treatment network. A nonconvex mathematical model (a mixed-integer nonlinear program, MINLP) is formulated to identify the layout of unit operations, stream assignments in the network, and operating conditions that minimize the treatment cost objective function.

Because of the nonconvexity of the problem, a branch-and-bound search algorithm is applied to obtain the global solution for the treatment network. The formulation of tight lower bounds is performed by approximating the nonconvex functions with piecewise underestimators and overestimators. In addition, several tightening constraints are added to facilitate the convergence of the proposed algorithm. An example of seawater desalination is presented as a case study to illustrate the proposed solution algorithm for the RO network global optimization.

Acknowledgment

The authors would like to acknowledge the financial support of the Natural Sciences and Engineering Research Council (NSERC) of Canada.

Nomenclature

Sets

SC = set of components present in each wastewater stream
SFPER = set of final permeate streams
SFREJ = set of final reject streams
SIN = set of inlet wastewater streams
SPU = set of pumps in the superstructure
SRO = set of RO stages
SROPER = set of permeate streams from the SRO
SROREJ = set of reject streams from the SRO
STU = set of turbine units
DIS1 = set of discrete intervals for a concave function
DIS2 = set of discrete intervals for domain q in a bilinear function χ
DIS3 = set of discrete intervals for domain w in a bilinear function χ

Parameters/Variables

$a_{pu,\mathrm{fx}}$ = fixed cost coefficient for a pump *pu* ($/(((kg/s) bar)$^{0.79}$ yr))
$a_{tu,\mathrm{fx}}$ = fixed cost coefficient a turbine unit *tu* ($/(((kg/s) bar)$^{0.47}$ yr))
$a_{pu,\mathrm{op}}$ = operational cost coefficient for a pump unit *pu* ($/(((kg/s) bar) yr))
$a_{tu,\mathrm{op}}$ = operational cost coefficient for a turbine unit *tu* ($/(((kg/s) bar) yr))
$a_{ro,\mathrm{m}}$ = cost coefficient of the RO module *ro* ($/(module yr))
$F_{\mathrm{i},mx}$ = inlet stream to a mixer node *mx* (kg/s)
F_{in} = inlet wastewater stream to the inlet node *in* (kg/s)
$F_{in-fper}$ = wastewater stream from the inlet node *in* to pump node *fper* (kg/s)
$F_{in-frej}$ = wastewater stream from the inlet node *in* to pump node *frej* (kg/s)
F_{in-spu} = wastewater stream from the inlet node *in* to pump node *pu* (kg/s)
F_{mx} = flow from mixer node *mx* (kg/s)
$F_{o,sp}$ = exit stream from a splitter node *sp* (kg/s)
F_{FPER} = final product permeate stream *fper* (kg/s)
F_{pu} = feed stream to the pump node *pu* (kg/s)
F_{pu-ro} = wastewater stream from *pu* to *ro* (kg/s)
F_{roper} = product permeate stream *roper* from *ro* (kg/s)
$F_{roper-fper}$ = permeate stream from *roper* to *fper* (kg/s)
$F_{roper-pu}$ = wastewater stream from the inlet node *roper* to pump node *pu* (kg/s)
F_{rorej} = product reject stream *rorej* from *ro* (kg/s)
$F_{rorej-frej}$ = reject stream from *rorej* to *frej* (kg/s)
$F_{rorej-pu}$ = reject stream from *rorej* to *pu* (kg/s)
$F_{rorej-pu}$ = wastewater stream from the inlet node *rorej* to pump node *pu* (kg/s)
$F_{rorej-ro}$ = reject stream from *rorej* to *ro* (kg/s)
$F_{rorej-tu}$ = reject stream from *rorej* to *tu* (kg/s)
F_{sp} = feed stream to a splitter *sp* (kg/s)
F_{tu} = feed stream to a turbine unit *tu* (kg/s)
$F_{tu-fper}$ = permeate stream from *fper* to *tu* nodes (kg/s)
$F_{tu-frej}$ = reject stream from *tu* to *frej* nodes (kg/s)
F_{tu-ro} = wastewater stream from *tu* to *ro* nodes (kg/s)
$\mathrm{Gap}_{\mathrm{node}}$ = gap for any node in the search tree
K_{c} = solute permeability coefficient (kg/(m^2 s))
l = fiber length (m)
l_{s} = fiber seal length (m)
NMd_{ro} = number of parallel modules in RO stage *ro*
OS = the osmotic pressure coefficient (bar/kg/kg)
P_{mx} = mixer output stream pressure value (bar)
PPu_{pu} = power consumption in pump stage *pu* (kg/(s bar))
P_{ro} = inlet feed pressure to a RO stage *ro* (bar)
PTu_{tu} = power production by a turbine unit *tu* (kg/(s bar))
q, w = independent variables of a bilinear function χ
r_{i} = inner radius of the hollow fiber (m)
r_{o} = outer radius of the hollow fiber (m)
SA = RO module surface area (m^2)
W = water permeability coefficient (kg/(s N))
$X_{c-\mathrm{avg},ro}$ = average concentration of component *c* on the feed side of the RO module
$X_{c,ro}$ = feed concentration of component *c* at RO stage *ro*
$X_{c,roper}$ = concentration of component *c* in any permeate stream *roper*
$X_{c,rorej}$ = reject concentration of component *c* in a reject stream *ro*
$X_{pc,\mathrm{SRO}}$ = permeate concentration of component *c* in RO stage *ro*
$y_{i,mx}$ = binary variable which define a stream assignment to a mixer node *mx*
ymix_{pu} = binary variable defines a mixing condition in eq 45
y_{PL} = binary variable which define permeate looping within the network
y_{pu} = binary variable for a pump unit *pu*
y_{tu} = binary variable for a turbine unit *tu*
y_{ro} = binary variable to define the existence of RO stage *ro*
z = an independent variable of a concave function $\psi(z)^{\alpha}$

Greek Letters

α_{pu} = fractional constant in the fixed cost of a pump *pu*
α_{tu} = fractional constant in the fixed cost of a turbine unit *tu*

γ = parameter defined by eq 7
η = parameter defined by eq 8
μ = viscosity of water (kg/(s m))
π_{ro} = osmotic pressure in a RO stage *ro* (bar)
$\psi(z)^{\alpha}$ = concave function
$\underline{\psi}(z)$ = underestimation of a concave function as defined by eq 24
χ = bilinear function
ω_{dis1} = binary variable which define the existence of a subinterval dis1
$\tau_{dis2,dis3}$ = binary variable defines the existence of a bilinear function value within the domains dis1 and dis2

Literature Cited

(1) El-Halwagi, M. M. Synthesis of reverse osmosis networks for waste reduction. *AIChE J.* **1992**, *38*, 1185−1198.

(2) El-Halwagi, M. M. Optimal design of membrane-hybrid systems for waste reduction. *Sep. Sci. Technol.* **1993**, *28*, 283−307.

(3) Vyhmeister, E.; Saavedra, A.; Cubillos, F. A. Optimal synthesis of reverse osmosis systems using genetic algorithms. Presented at European Symposium on Computer-Aided Process Engineering-14, 2004.

(4) Saif, Y.; Elkamel, A.; Pritzker, M. Optimal design of reverse-osmosis networks for wastewater treatment. *Chem. Eng. Process.* (in press, DOI: 10.1016/j.cep.2007.11.007).

(5) Zhu, M.; El-Halwagi, M. M.; Al-Ahmad, M. Optimal design and scheduling of flexible reverse osmosis networks. *J. Membr. Sci.* **1997**, *129*, 161−174.

(6) Maskan, F.; Wiley, D. E.; Johnston, L. P. M.; Clements, D. J. Optimal design of reverse osmosis module networks. *AIChE J.* **2000**, *46*, 946−954.

(7) Evangellsta, F. A short cut method for the design of reverse osmosis desalination plants. *Ind. Eng. Chem. Process Des. Dev.* **1985**, *24*, 211−223.

(8) Weber, W. *Physiochemical Processes for Water Quality*; Wiley: New York, 1972.

(9) McCormick, G. P. Computability of global solutions to factorable nonconvex programs. Part I—Convex Underestimating Problems. *Math. Prog.* **1976**, *10*, 146−175.

(10) Sherali, H. D.; Alameddine, A. A new reformulation−linearization technique for bilinear programming problems. *J. Global Opt.* **1992**, *2*, 379−410.

(11) Meyer, C. A.; Floudas, C. A. Global optimization of a combinatorially complex generalized pooling problem. *AIChE J.* **2006**, *52*, 1027−1037.

(12) Karuppiah, R.; Grossmann, I. E. Global optimization for the synthesis of integrated water systems in chemical processes. *Comput. Chem. Eng.* **2005**, *30*, 650−673.

(13) Brooke, A.; Kendrik, D.; Meeraus, A. *GAMS User's Guide*; Boyd & Fraser Publishing Co.: Danvers, MA, 1992.

Received for review September 29, 2007
Revised manuscript received February 12, 2008
Accepted February 26, 2008

IE071316J